Available online at www.sciencedirect.com
ScienceDirect
C. R. Physique 7 (2006) 931–941
COMPTES RENDUS PHYSIQUE
http://france.elsevier.com/direct/COMREN/

Ultimate lithography/Lithographie ultime

Advanced metrology needs for nanoelectronics lithography

Stephen Knight *, Ronald Dixson, Ronald L. Jones, Eric K. Lin, Ndubuisi G. Orji, R. Silver, John S. Villarrubia, András E. Vladár, Wen-li Wu

National Institute of Standards and Technology, 100 Bureau Drive, Gaithersburg, MD 20899, USA

Abstract

The semiconductor industry has exploited productivity improvements through aggressive feature size reduction for over four decades. While enormous effort has been expended in developing the optical lithography tools to print ever finer features, significant advances have also been required to measure the printed features. In this article we will discuss the current state of the art in the metrology for measuring critical dimensions of printed features for scanning electron microscopy and atomic force microscopy, and describe work at the National Institute of Standards and Technology advancing these tools as well as exploratory work on two new promising techniques, scatterfield microscopy and small angle X-ray scattering. Line width roughness critical dimension and overlay metrology and control are two of the most significant industry needs mentioned in the International Technology Roadmap for Semiconductors (2005). ***To cite this article: S. Knight et al., C. R. Physique 7 (2006).***
Published by Elsevier Masson SAS on behalf of Académie des sciences.

Résumé

Besoins en métrologie avancée pour la lithographie nanoélectronique. Depuis plus de quatre décennies l'industrie du semiconducteur a mis à profit les améliorations de productivité obtenues par le biais d'une réduction agressive des dimensions de motifs. Alors qu'un effort énorme a été dépensé pour développer les outils de lithographie optique afin d'imprimer des traits de plus en plus fins, des avancées significatives ont été aussi nécessaires pour mesurer les motifs imprimés. Dans cet article nous discuterons certaines techniques de pointe de métrologie utilisées aujourd'hui pour mesurer les dimensions critiques de traits imprimés à savoir la microscopie électronique à balayage et la microscopie à force atomique. Nous décrirons le travail mené au National Institute of Standards and Technology pour faire progresser ces instruments, ainsi que le travail exploratoire sur deux techniques nouvelles prometteuses que sont la microscopie en champ diffracté et la diffraction de rayons X aux petits angles. La métrologie et le contrôle de la rugosité de trait, des dimensions critiques et du recouvrement sont deux des besoins les plus importants de l'industrie auxquels fait référence la feuille de route internationale de la technologie des semiconducteurs (2005). ***Pour citer cet article : S. Knight et al., C. R. Physique 7 (2006).***
Published by Elsevier Masson SAS on behalf of Académie des sciences.

Keywords: CD-SEM; CD-AFM; Scatterfield microscopy; CD-SAXS

Mots-clés : CD-SEM ; CD-AFM ; Microscopie en champ diffracté ; CD-SAXS

* Corresponding author.
E-mail address: stephen.knight@nist.gov (S. Knight).

1631-0705/$ – see front matter Published by Elsevier Masson SAS on behalf of Académie des sciences.
doi:10.1016/j.crhy.2006.10.004

1. Introduction

Dimensional metrology is a key metrology essential for maintaining process control in integrated circuit manufacturing [1,2]. Currently scanning electron microscopy and optical scatterometry are the mainstream metrology tools for gate stack, source-drain via, and interconnect metrology, primarily because of high through-put. Atomic force microscopy is used in special metrology situations, primarily because of its ability to extract unambiguous three-dimensional information. Scatterfield microscopy and critical dimension small angle X-ray scattering are emerging metrology techniques that hold promise for future in-line, at-line or perhaps even in situ metrology tools for process monitoring and process control.

Critical dimension (CD) metrology tools can be divided into two classes:

- The first class includes those tools that provide direct high spatial resolution images of the measured structures. This class includes scanning electron microscopy (SEM) and atomic force microscopy (AFM). The images may (generally do) contain artifacts that require modeling for interpretation, but the distinguishing characteristic of techniques in this class is that the sample volume that contributes signal to a measurement is small, with size comparable to or smaller than the individual structures being measured.
- The second class consists of tools in which the measurement volume encompasses a periodic array of nominally identical structures. This class includes optical scatterometry, optical scatterfield microscopy, and small angle X-ray scattering. The signal from these techniques is not an image of an individual structure, but is a scatter signal that is interpreted, via a model, to determine average shape and size parameters of the structures comprising the array.

Tools from each of these classes have complementary roles to play. The strong suit of techniques in the second class is provision of highly repeatable (and possibly, if the models can be shown to be good, accurate) measurements of average dimensions of test patterns. Information from all structures is collected in parallel; this has the potential, realized in the case of the optical techniques, of making the methods fast. On the other hand, the very averaging that produces these advantages represents a disadvantage when it is not the average feature but the outlier that is of interest. Techniques in the first class can image individual structures, so are as able to measure outliers (e.g., the narrowest, leakiest gate) as average features. They can measure actual circuit features (which are generally not in periodic arrays) in situ in addition to special test structures. However, data collection for these techniques is generally serial, so they are slower than the fastest area-averaging methods of class 2 for determining large-area averages. These, along with other advantages and disadvantages of the methods, are summarized in Table 1.

Table 1
Comparison of Critical dimension (CD) metrology tools

Method	Strength	Weakness
Scanning Electron Microscopy	High throughput; measures both repeating and individual structures; measures line edge roughness (full probability distribution) [2]	Requires vacuum; hydrocarbon contamination; photoresist shrinkage; requires simple modeling
Atomic Force Microscopy	Measures both repeating and individual structures; measures sidewall surfaces, roughness (full probability distribution)	Low throughput; tip-wear and crashes; modeling for tip deconvolution required
Optical Scatterometry	High throughput; non-destructive; measures average of many lines	Requires complex modeling; requires special metrology targets
Optical Scatterfield Microscopy	High throughput; non-destructive; measures average of many lines; simultaneous overlay; small target size	Immature technology; requires complex modeling; requires special metrology targets
Small Angle X-ray Scattering	Accurate; overlay of hidden features; line edge and width roughness (standard deviation only); measures average and variance over multiple lines, simple analysis	Need of high brightness sources which are only synchrotrons; lab sources are 3 orders of magnitude less bright; requires metrology targets larger than those for optical scatterometry

In the following sections we will discuss briefly the current state of the art and current developments in critical dimension scanning electron microscopy, atomic force microscopy, and discuss exploratory work in scatterfield microscopy and small angle X-ray microscopy applied to critical dimension metrology.

2. Scanning Electron Microscopy for critical dimension metrology

2.1. Current status

Dimensional metrology for nanostructures requires the measuring instruments to provide shape and size information with atomic levels of resolution and precision. In production this has to be done within a few seconds. The scanning electron microscope (SEM) is one of the indispensable imaging and measurement instruments that can achieve this performance. In the best cases the SEM can image structures with close to 1 nm spatial resolution, and its measurement resolution (i.e. the ability to tell apart different structures) can be better than 1 nm [3]. SEMs provide information on both isolated and repeating structures with better than 1 nm measurement precision. Nevertheless, existing SEMs cannot achieve this excellent performance on all possible structures because there are significant, but not insurmountable problems to solve. On one hand, all instrument and measurement parameters have to be optimized and monitored so they do not drift from the optimum settings; on the other hand, new, more sophisticated hardware and software have to be developed. Many of these are already in existence but not yet implemented in easy-to-use ways. Substantial improvements are possible, and these could make SEMs meet future requirements.

The SEM is one among several instruments that can provide information necessary in the development of nanoelectronics devices and in the control of their manufacturing process. These instruments may provide unique or similar information. In order to gain confidence in their results, comparisons are inevitable. To compare meaningfully the results of various metrology methods, it is necessary to know the limits of their validity and to account properly for all important measurement uncertainty components. Otherwise, the reliability of these comparisons would be unknown. This could lead to erroneous device designs, and/or loss of control of the manufacturing processes.

2.2. Tool improvements

New SEM technology can significantly improve spatial resolution by using brighter and more monochromatic electron guns. The use of nano-tips as emitters and electron energy filters will deliver superior performance [4]. More sophisticated electron-optical columns with adaptive, highly accurate, automatic astigmatism and beam focus control and aberration corrected lenses will also further improve the spatial resolution. Automatic (better than 1 nm) landing position control and compensation for sample stage vibration and drift will be necessary to avoid resolution deterioration. Automatic column control, performance monitoring, optimized and known instrument and electron probe parameters will be used in the collection of data and in fully optimized, highly accurate, model-based metrology.

In the case of high vacuum SEMs, contamination of the sample is an issue. However, it is possible to reduce significantly the contamination problem by occasionally cleaning the sample stage and chamber by the use of low-energy oxygen plasma [5].

2.3. Image modeling

The use of highly accurate, three-dimensional models is indispensable. For reliable results when the information volume (i.e. where the collected information originates) comparable to or larger than the needed resolution, models are necessary. The models will be based on thorough understanding of the governing physical processes of the interaction of the electron beam and the sample and the instrument itself. The arbitrary algorithms that are in use today will not be able to provide the needed precision, accuracy and sensitivity to the variations of the samples. Model-based metrology methods have shown superior performance in both measurement resolution and bias [6]. With new, fast computers the generation of the modeled, simulated signals will be done in a matter of a few minutes, and this will not hold back the SEM-based measurements in any significant way. The currently available Monte Carlo simulation methods have shown that it is realistic to obtain significantly better results and to generate the modeled line scans and even images within a matter of seconds. Models will include not just the generation of signals, but will account for all aspects of

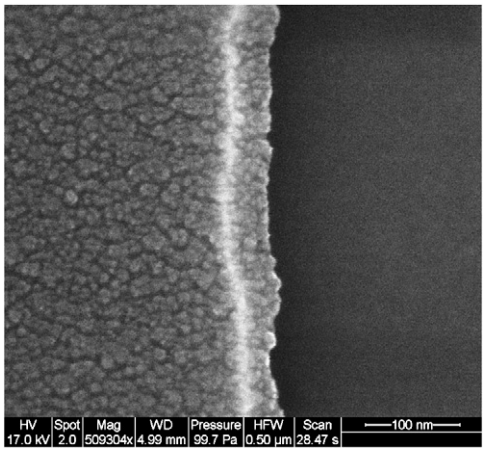

Fig. 1. SEM micrograph of a phase shifting photomask. The field of view is 500 nm. (Courtesy of Milos Toth of FEI Co.)

the signal formation, including the electro-magnetic fields above the sample and within the column, and all pertinent instrument parameters related to the detectors and the signal chain.

2.4. Variable pressure SEMs

It will be inevitable to deal with the problems of sample charging, sample damage, and contamination. While these cannot be fully eliminated, all of them can be kept at levels that allow for good results. For example, with variable pressure SEMs it has been demonstrated that suitable charge control and excellent spatial resolution can be achieved on photomask samples [7]. These, due to sample charging, are typically difficult to measure. Fig. 1 shows the SEM image of a portion of a phase shifting photomask taken at 500 000 times magnification with 17 kV accelerating voltage. The sample charging even at this high accelerating voltage is acceptable, and the Cr grain structure is clearly resolved. This is only possible because the SEM was operated in close to 100 Pa water vapor. These SEMs deposit much less carbonaceous contamination than high-vacuum SEMs, and may actually leave the sample cleaner.

3. Atomic Force Microscopy for critical dimension metrology

3.1. Current status

Critical dimension atomic force microscopy (CD-AFM) was first developed by Martin and Wickramasinghe [8] at IBM. Their technology was subsequently marketed as the first generation of a commercially available instrument.

The most significant differences between CD-AFM and conventional or top-down AFM are that surface sensing occurs along both lateral and vertical axes and that flared tips are used—which allows vertical and even somewhat reentrant structures to be accurately measured. A conceptual illustration of CD-AFM is shown in Fig. 2.

Since the advent of commercial CD-AFM technology, these tools have gained modest acceptance in semiconductor manufacturing for process development and to support in-line CD metrology. The most common application of CD-AFMs has been to support CD-SEM metrology as a reference for tool matching or as a non-destructive alternative to TEM and SEM cross-sections [9–13]. There has also been significant use of CD-AFMs to study the properties of edges and sidewalls—specifically the line edge roughness (LER) [14,15].

3.2. Uncertainty, calibration, and standards

Since 2001, there has been an extensive collaboration between NIST and SEMATECH to perform traceable calibration of CD-AFM metrology and reduce measurement uncertainties. The center piece of this fruitful partnership has been the implementation of a CD-AFM based reference measurement system (RMS) at SEMATECH [16–20].

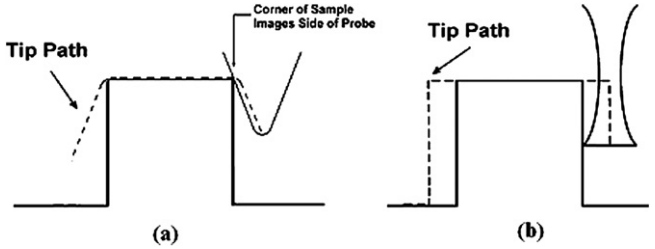

Fig. 2. Illustration of differences between (a) conventional AFM and (b) CD-AFM. In conventional AFM, the apparent width of a structure includes a tip-induced dilation that is a function of height. In a CD-AFM most of the tip-induced dilation in the apparent width consists of a constant term—the zeroth order component.

The accuracy of pitch and height measurements using CD-AFM depends primarily upon traceable calibration of the scales—which correspond to stage displacement in these instruments. There are a variety of pitch and height standards available that may be used for such calibration—including some available from NIST and equivalent national metrology institutes (NMIs) in other nations.

Although the analysis of uncertainty is different for every measurement and will exhibit some dependence on the specific sample and tip, it is possible to make general statements about limits and achievable levels of uncertainty. For the CD-AFM/RMS at SEMATECH, standard uncertainties as low as 0.1% have been demonstrated for pitch measurements in the range of several micrometers; for step height measurements, standard uncertainties at the level of 0.2% have been demonstrated on step heights of several hundred nanometers [21].

Although there are many important metrology applications of CD-AFM in semiconductor manufacturing, the most common is linewidth metrology—for measurement of gate CD or as a reference tool for in-line critical dimension scanning electron microscopes (CD-SEMs). For this application, it is especially important to minimize the uncertainty of the CD-AFM width measurements.

Although the uncertainties in pitch measurements apply to width measurements as well, these are not typically the most significant terms for deep submicrometer linewidth measurements. Instead, the most challenging source of uncertainty in width measurements is the calibration of the tip width and shape.

Although the interaction of an AFM tip with the imaged surface is complex, for many purposes a highly simplified and two-dimensional model illustrated in Fig. 2 can be useful. In this basic model, the effect of the tip is represented as a simple additive offset which must be subtracted from the apparent width to obtain an accurate measurement. The uncertainty in the value of the tip width to subtract is sometimes referred to as the zeroth order tip width uncertainty.

The finer details of the tip-sample interaction, pertaining to things like flare radius, feature sidewall angle, feature corner radius, and the three-dimensional nature of both the tip and sample (i.e., shape in the axis not shown) are thought of as being higher-order tip effects. The idealized geometry of Fig. 2 does not incorporate any of these considerations. While higher order effects can be important in the measurement of less uniform structures such as photoresist lines, these effects are often negligible for measurement of relatively uniform structures—particularly those with near-vertical sidewalls.

For many years, CD-AFM users typically developed in-house reference standards for tip width calibration—often based on SEM or TEM cross sections. But, the uncertainty of such standards was often significant or uncharacterized. Tip characterizer samples—which used a sharp ridge to calibrate the tip width—are commercially available. However, scanning such samples can result in tip damage, and the uncertainty of tip calibrations based on this method is limited to about 5 nm.

The NIST response to this pressing need for more accurate CD-AFM tip calibration was the development of single crystal critical dimension reference materials (SCCDRMs) [21–25]. These specimens, which are fabricated using a lattice plane selective etch on (110) silicon, exhibit near vertical sidewalls and high uniformity. As a result of this project, CD-AFM tip width can now be calibrated with 1 nm standard uncertainty.

Following this dramatic reduction in the uncertainty of tip width calibration, the frontier of CD-AFM width metrology now lies in the understanding and correction for higher order effects resulting from the tip shape. Developments in this area are continuing at NIST with experiments to assess the performance of tip shape characterizers and image reconstruction algorithms.

4. Scatterfield microscopy for critical dimension and overlay metrology

4.1. Introduction

Recently, there has been significant research investigating potential alternative technologies for overlay measurement beyond the 65 nm node. This work has often focused on meeting the challenges of imaging very small device-sized targets for improved overlay measurements [26,27]. Tighter overlay tolerances are driving the need to use device-sized targets, which more closely emulate the characteristics of the actual features of interest printed on the wafers. The move to more sophisticated overlay targets is being explored in several leading edge manufacturing environments.

In previous publications we have described the implementation of the scatterfield microscopy technique, which generally involves engineering the illumination in combination with structured samples [28,29]. To investigate the limitations of this approach we have modeled targets with linewidth dimensions down to 10 nm. Fundamentally there are no significant roadblocks to measuring isolated features $1/20$th the size of the measurement wavelength and, using well engineered illumination and target designs, very good signal-to-noise ratios can be achieved. A number of examples presented in [30] utilize both theoretical techniques and experimental implementations to develop and demonstrate excellent optical response to very small features. The problem, however, becomes more challenging when the features become densely positioned.

4.2. Zero order imaging

We have developed a new approach to measure very dense arrays optically. As an example, we analyze 50 nm sized features which are spaced 250 nm apart with 546 nm wavelength light. The typical optical response in this case at 546 nm measurement wavelength is a flat intensity pattern with no optical intensity variation. The cause of this is that only specular or zero-order light is reflected. That is, the collection optics are only capturing the specular reflected component and either higher order terms do not exist or they are outside the collection aperture. We have developed an approach to image the sample in this situation. If features are placed close enough together they locally reflect only the zero order component. This results in a flat intensity response as a function of position across the image plane. However, if the target actually has a finite overall dimension within the field of view, then the edges of the target will reflect higher order light. We refer to this as zero order imaging.

The result is that small groupings of features with very sub-wavelength dimensions can give excellent localized optical response. Their optical response is a combination of the higher order edge response and a zero order central intensity. These targets can be designed for use as overlay targets, but also have the potential for use in linewidth metrology, as discussed shortly. For overlay applications the arrayed targets can act as individual objects which are well suited for edge detection algorithms and correlation functions commonly used to determine relative feature positions with image based overlay techniques.

4.3. Back focal plane scanning

In addition to the imaging of dense features as described above, a more complex approach is to use an aperture, which is scanned in a conjugate back focal plane resulting in illumination of the sample at specific chosen angles. The images captured are the result of two different phenomena. Either a dense array is imaged and only a constant intensity is captured at the image plane, or for less dense targets the image will contain higher order optical response information and appear like a conventional optical image of an array. In either case, the intensity image is captured and a total or average intensity as a function of illumination angle or aperture position is determined. The hardware and instrumentation used in the research reported in this paper are described in detail elsewhere [31].

4.4. Full field angle scanning

In the first part of this section the data described were acquired from arrays, fabricated with the SEMATECH Overlay Metrology Advisory Group version 3 reticle set, which fills the field of view. The data were acquired by collecting conventional images at the image plane with a CCD camera. A window or kernel is placed in the image and

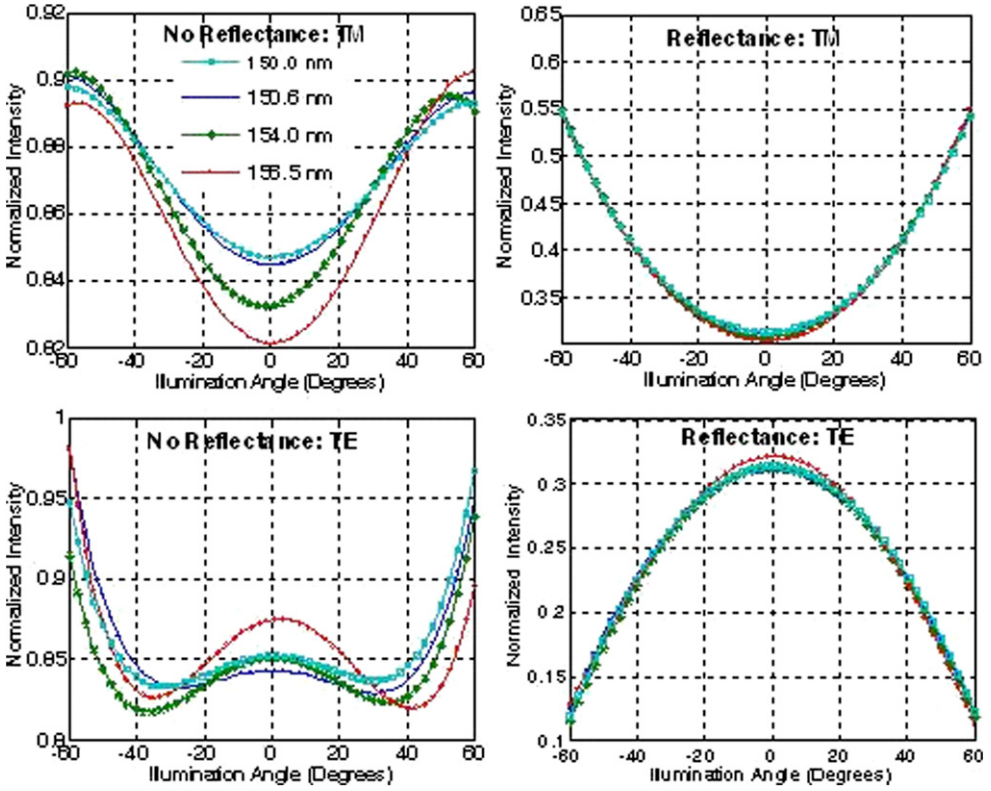

Fig. 3. TM polarization is on top and TE is shown on the bottom. The vertical axes are normalized intensity and the horizontal axes are illumination angle. The data show good sensitivity to nm changes in linewidth. The image has been normalized to the background.

an average intensity per unit area determined. This mean intensity is evaluated for each angle of illumination. Two types of results are observed. The first result occurs when the pitch values are large enough for higher-order optical information to be scattered and collected by the optics. The second, alternative result is a flat intensity across the field containing only zero-order optical information. The aperture is scanned in the back focal plane across a large enough distance to clip the aperture at the extremes and as a result the intensity falls off for positions in the back focal plane which correspond to angles of illumination greater than 60°.

Fig. 3 shows two sets of curves on the left, one for *p* polarization and one for *s* polarization data. This figure shows a 300 nm pitch array with linewidths varying from 150 to 156.5 nm based on the SEM values. The data shown on the left side of the figure are not yet normalized for silicon reflectivity although they have been processed for background and dark current compensation. The curves show a clear sensitivity to nm changes in linewidth. These data are repeatable and show a monotonic response to linewidth changes.

The data on the right side of Fig. 3 show the same results after they have been corrected for the silicon reflectivity. The correction effectively scales the data, which in this case, increases the dynamic range in the graph, and makes the curves appear closer to each other in value relative to the raw uncorrected data.

4.5. High resolution overlay targets

Although the above discussion and results were focused on sensitivity to changes in linewidth, geometry, and the ability to image small features, these results have significant implications for overlay metrology. A key difference between linewidth measurements and overlay measurements is that linewidth analysis has routinely used theoretical modeling to determine threshold values for edge detection algorithms or measurements fully based in model results such as scatterometry. On the other hand, overlay metrology has been exclusively an optical image based technique with modeling only used off line and for optimization purposes. In this section we will apply the same scanning aperture techniques to an array of targets within the field of view.

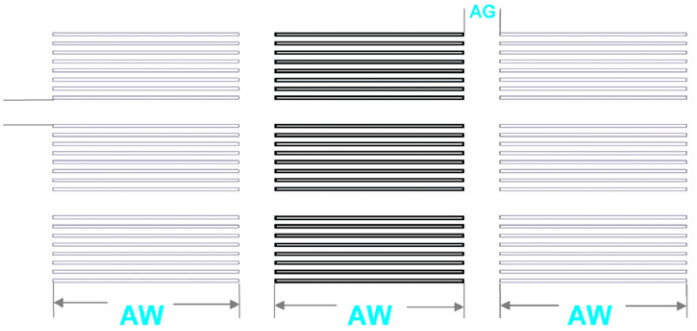

(a)

- Two sets of targets:
  - 1) This shows equal lines and spaces.
  - 2) A similar set of targets but with different linewidths for each group of 8 lines. The linewidths span typical process variation windows.
- AW = 2.5 um and 5.0 um
- AG = 1.0 um
- 5 different pitches and 3 offset values: 0, +/ - 10 nm

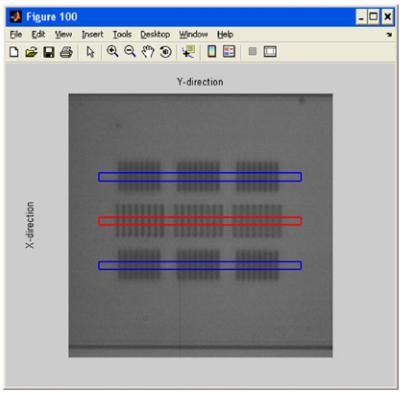

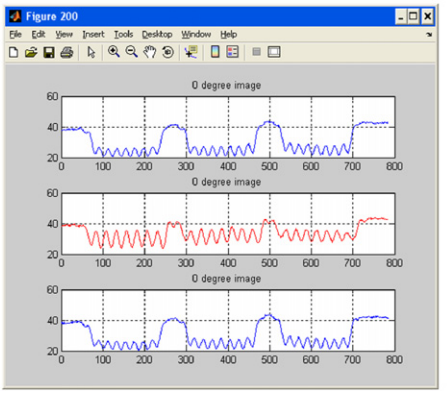

(b)
LITO
90nm 1:3

Fig. 4. A schematic of the target designs is shown in (a). This is one example of several variations of this design. The lower part of the figure shows an image and a set of profiles for a target which reflects higher-order optical content. LITO is an acronym to identify a two level line inner trench outer process. In (b), the upper and lower line sets are from process level 1 and the inner line sets are from a different photolithographic level, process level 2.

A set of targets was designed to test this approach which consisted of an array of small line arrays as shown in Fig. 4. Unlike the previous targets, these targets are intended to allow measurement of overlay between two layers with a set of targets that can also be imaged using the zero order imaging approach. In the figure, the outer line sets are from one photolithographic level and the inner line sets are from a second photo level. The current target designs were for sets of eight lines with a variety of line lengths, line set separations, and line widths to allow investigation of these parameters on target performance. This figure shows one variation of the target design. These more complex targets were design to allow imaging in two different modes. In the first mode the optical response to individual line sets includes high-order optical content reflecting from the central part of the lines as shown in Fig. 4(b). In the second mode, the line density is such that only the zero order is reflected from the central region of the target, which is known as the zero order imaging mode.

4.6. Scanning overlay target measurements

The arrayed overlay targets can also be used for arrayed linewidth analysis. Acquiring data by scanning the illumination angle and acquiring images as the aperture is incremented across the back focal plane allows the entire set of line arrays to be analyzed simultaneously. Using the approach described above with these targets enables simultaneous analysis of the nine line arrays. We have used this approach to analyze target designs with array increments of 5 nm and average nominal CDs of 55, 60 and 65 nm. From this image an average intensity is determined for the central region for each profile. Both the experimental results and simulation data show approximately 10 percent changes in the integrated intensity each increment in linewidth. These targets designs are interesting in that they have applications for both image-based overlay metrology and simultaneously for use in linewidth metrology.

5. Critical dimension small angle X-ray scattering metrology

It is well documented that current measurement methods for dimensional metrology, electron microscopy and optical scatterometry, face significant challenges as the minimum feature size in semiconductor devices approaches sub-35 nm length scales. To meet this challenge, we have developed a scattering method using X-rays termed critical dimension small angle X-ray scattering (CD-SAXS). There are several advantages to the use of X-rays as a probe in this application. First, the use of X-rays with a wavelength less than 0.1 nm provides a higher measurement resolution than any optical based metrology. Second, the refractive index of all materials at this wavelength, including metals and ceramics, is close to unity. As a result, X-ray scattering data can be analyzed using straightforward Fourier transforms. Third, most materials are relatively transparent to these X-rays and scattering data can be collected with a simple transmission geometry. Finally, the penetration power of these X-rays is sufficient to enable the measurement of buried structures non-destructively.

In a CD-SAXS measurement (Fig. 5), a monochromic and highly collimated X-ray beam travels through a patterned sample with periodic structure and is scattered onto a 2-dimensional detector. The scattered intensity is recorded as a function of scattering angle, 2θ, and converted to a scattering vector, $q = 4\pi/\lambda \sin(\theta)$, where λ is the X-ray wavelength. The observed intensity distribution is related to the 3-dimensional Fourier transform of the pattern and can be analyzed to quantify the shape of the average pattern cross-section as well as the variance in its dimensions in the scattering volume. Dimensional information along the thickness direction of the patterns, can be obtained by collecting scattering data at various sample rotation angles [32,33].

To demonstrate the analysis needed to quantify the shape of line/space patterns, we model the cross-section of the line as a trapezoid as shown in Fig. 6. Fig. 7 shows both the real space coordinate axes and its presentation in the Fourier space. The form of the Fourier transform of the trapezoid is useful because information about the sidewall angle and the average line height are immediately visible from the angle between diverging intensity streaks and the spacing between parallel intensity streaks. The relationships needed to quantify sidewall angle and line height are shown in Fig. 7.

Experimental CD-SAXS data from a test line grating is given in Fig. 8. The data resemble closely the model calculation shown in Fig. 7. We note that the data in Fig. 8 is an algebraic product of the lattice which defines the arrangement of the lines and the cross-section of individual line. As a result, the periodicity of the line grating as well as the line width can be determined from the data along q_x at $q_z = 0$. The dimensions measured from this sample are: pitch $= 330.5 \pm 0.5$ nm, line width $= 160 \pm 1$ nm, height $= 460 \pm 10$ nm and sidewall angle $= 5.6 \pm 0.5$ deg.

In addition to the pitch and line shape parameters, we have extended this analysis to quantify other important parameters describing the pattern cross-section such as line-edge roughness (LER), line-width roughness (LWR), vertical standing waves within a resist, two dimensional arrays of via holes, and sidewall density profiles of nano-patterned low-k dielectrics. Current work is focused on developing models for structures with more complicated, arbitrary cross sections and for the analysis of roughness covering different spatial frequency modes.

To date, CD-SAXS measurements show tremendous promise towards meeting the dimensional metrology needs of the semiconductor industry at future technology nodes. When applied to periodic structures on silicon, the use of short

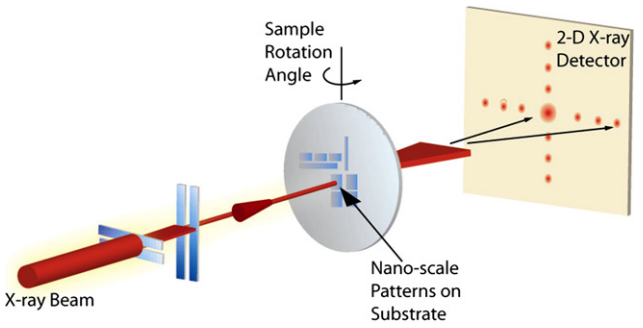

Fig. 5. Schematic of the CD-SAXS geometry used in this work, showing the X-ray beam (solid line) in transmission through the patterned sample, the scattering angle, 2θ, and the axis of sample rotation for line gratings is along the line direction.

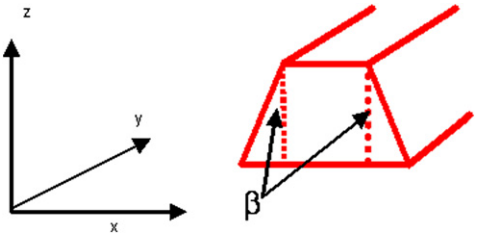

Fig. 6. The trapezoid cross-section of model line/space patterns.

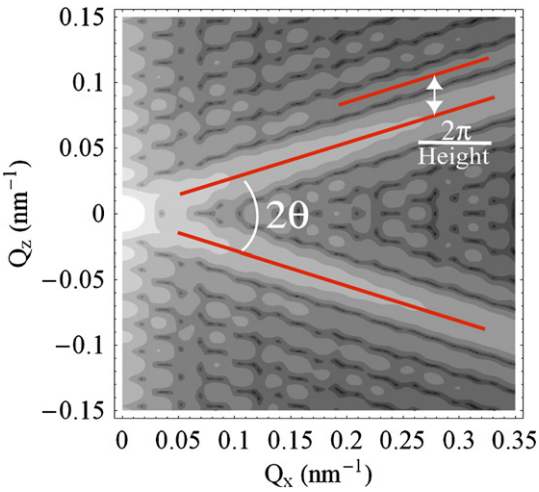

Fig. 7. Schematic of lines with trapezoid cross-section in both real space and Fourier space, where intensity streaks form an angle equivalent to twice the sidewall angle, and the distance between satellite streaks is inversely proportional to the pattern height, H.

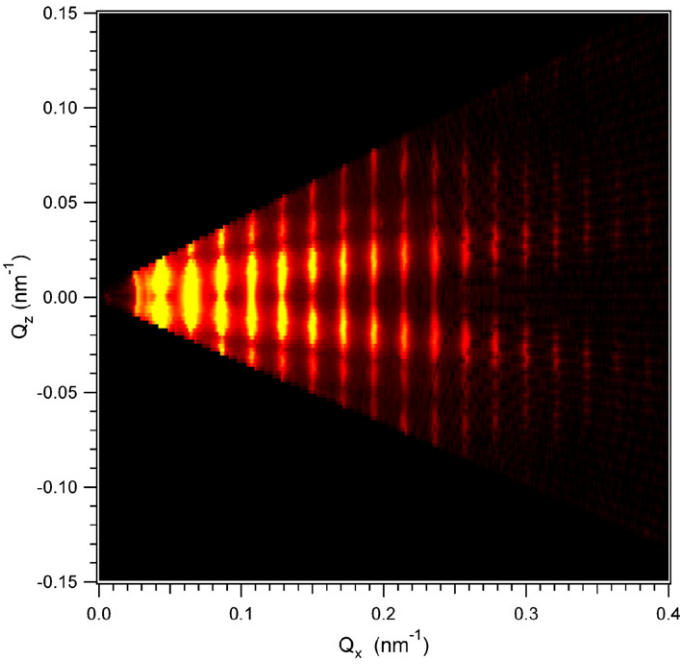

Fig. 8. Experimental results of a photoresist line grating expressed in the q_x–q_z plane.

wavelength X-rays in a transmission geometry allows rapid quantification of the pitch, line-width, sidewall angle, line-height, and the average line cross-section. Straightforward models have been developed to quantify LER, LWR, and density profiles. Further, these measurements do not require any additional sample preparation, are non-destructive, and can measure buried structures of different materials.

The major drawback to CD-SAXS is the lack of X-ray generators with sufficient brightness for on-line fab line metrology. The intensity form current X-ray generators remains (3 to 5) orders of magnitude below that needed for in-line inspection by semiconductor industry. The results shown in this work were obtained from a high intensity synchrotron source at the Advanced Photon Source of Argonne National Laboratory. The shorter term role of CD-SAXS may be its application as a laboratory scale tool that can be used to calibrate optical and SEM based measurements, to characterize new materials and processes, or to help optimize existing measurement methods. For these laboratory-scale applications, NIST has designed and installed a high resolution CD-SAXS facility using a rotating anode X-ray source.

6. Concluding remarks

Continued progress in tool development will enable SEMs to be used for the foreseeable future and will be able to provide indispensable information for nanoelectronics. The introduction of the variable pressure SEM will greatly enhance the ability to measure insulating structures such as masks.

A decade after its introduction, CD-AFM is now gaining widespread acceptance in semiconductor manufacturing metrology. At-line reference metrology is the most widespread application of this technology.

THE NIST single crystal critical dimension reference material (SCCDRM) project has resulted in a five-fold reduction of tip width calibration uncertainty in CD-AFM metrology. Consequently, the frontier of CD-AFM metrology now lies in accurate calibration of tip shape and correction of higher order tip effects.

Scatterfield microscopy development has shown rapid progress in the past few years, and is finding selective application in nanoelectronics manufacturing, particularly in overlay.

It has been demonstrated that in line gratings the pitch, line width, sidewall angle and line height can all be determined from the scattering of X-rays with a wavelength less than 0.1 nm without any sample preparation or the need

for complex model calculations. Intrinsically, X-ray based scattering is expected to have better spatial resolution than optical method since its wavelength is a few orders of magnitude smaller than that of the optical wave. The current effort is focused on the quantification of sidewall roughness both along the direction of the line and along the thickness direction.

References

[1] International Technology Roadmap for Semiconductors. 2005 edition available online at http://public.itrs.net/.
[2] J.S. Villarrubia, Issues in line edge and linewidth roughness metrology, in: D.G. Seiler, A.C. Diebold, R. McDonald, C.R. Ayre, R.P. Khosla, S. Zollner, E.M. Secula (Eds.), Characterization and Metrology for ULSI Technology, 2005, in: AIP Conference Proceedings, vol. 788, AIP Press, New York, 2005, p. 386.
[3] J.S. Villarrubia, A.E. Vladár, J.R. Lowney, M.T. Postek, Scanning electron microscope analog of scatterometry, Proc. SPIE 4689 (2002) 304–312.
[4] A.E. Vladár, Zs. Radi, M.T. Postek, D.C. Joy, Nanotip electron gun for the scanning electron microscope, Scanning 28 (3) (2005) 133.
[5] A.E. Vladár, M.T. Postek, R. Vane, Active monitoring and control of electron beam induced contamination, Proc. SPIE 4344 (2001) 835.
[6] J.S. Villarrubia, A.E. Vladar, M.T. Postek, A simulation study of repeatability and bias in the CD-SEM, Proc. SPIE 5038 (2003) 138–149.
[7] M. Toth, W.R. Knowles, Secondary electron imaging of nonconductors with nanometer resolution, Appl. Phys. Lett. 88 (2006) 023105.
[8] Y. Martin, H.K. Wickramasinghe, Method for imaging sidewalls by atomic force microscopy, Appl. Phys. Lett. 64 (1994) 2498–2500.
[9] B. Banke, C. Archie, M. Sendelbach, J. Robert, J. Slinkman, P. Kaszuba, R. Kontra, M. DeVries, E. Solecky, Reducing measurement uncertainty drives the use of multiple technologies for supporting metrology, Proc. SPIE 5375 (2004) 133–150.
[10] M.D. Lagerquist, W. Bither, R. Brouillette, Improving SEM linewidth metrology by two-dimensional scanning force microscopy, Proc. SPIE 2725 (1996) 494–503.
[11] K. Wilder, B. Singh, W.H. Arnold, Sub-0.35-micron critical dimension metrology using atomic force microscopy, Proc. SPIE 2725 (1996) 540–554.
[12] H.M. Marchman, N. Dunham, AFM: A valid reference tool?, Proc. SPIE 3332 (1998) 2–9.
[13] S.K. Yedur, B. Singh, Evaluation of atomic force microscopy: Comparison with electrical CD metrology and low voltage scanning electron microscopy, Proc. SPIE 3677 (1999) 43–52.
[14] S. Fuller, M. Young, Photomask edge roughness characterization using an atomic force microscope, Proc. SPIE 3332 (1998) 433–440.
[15] A. Kant, G. Taylor, N. Samarakone, Quantitative line edge roughness characterization for sub-0.25 um DUV lithography, Proc. SPIE 3677 (1999) 35–42.
[16] N.G. Orji, A. Martinez, R. Dixson, J. Allgair, Progress on implementation of a CD-AFM based reference measurement system, Proc. SPIE 6152 (2006) 61520O-1-12.
[17] R. Dixson, J. Fu, N. Orji, W. Guthrie, R. Allen, M. Cresswell, CD-AFM reference metrology at NIST and SEMATECH, Proc. SPIE 5752 (2005) 324–336.
[18] R. Dixson, A. Guerry, Reference metrology using a next generation CD-AFM, Proc. SPIE 5375 (2004) 633–646.
[19] R. Dixson, A. Guerry, M. Bennett, T. Vorburger, B. Bunday, Implementation of a reference measurement system using CD-AFM, Proc. SPIE 5038 (2003) 150–165.
[20] R. Dixson, A. Guerry, M. Bennett, T. Vorburger, M. Postek, Toward traceability for at line AFM dimensional metrology, Proc. SPIE 4689 (2002) 313–335.
[21] R.G. Dixson, R.A. Allen, W.F. Guthrie, M.W. Cresswell, Traceable calibration of critical-dimension atomic force microscope linewidth measurements with nanometer uncertainty, J. Vac. Sci. Technol. B 23 (2005) 3028–3032.
[22] M. Cresswell, R. Dixson, W. Guthrie, R. Allen, C. Murabito, B. Park, J. Martinez de Pinillos, A. Hunt, Critical dimension reference features with sub-five nanometer uncertainty, Proc. SPIE 5752 (2005) 288–303.
[23] R.A. Allen, M.W. Cresswell, C.E. Murabito, R.G. Dixson, E.H. Bogardus, Critical dimension calibration standards for ULSI metrology, in characterization and metrology for ULSI technology, AIP Conf. Proc. 683 (2003) 421–428.
[24] M.W. Cresswell, E.H. Bogardus, J.V. Martinez de Pinillos, M.H. Bennett, R.A. Allen, W.F. Guthrie, C.E. Murabito, B.A. am Ende, L.W. Linholm, CD reference materials for sub-tenth micrometer applications, Proc. SPIE 4689 (2002) 116–127.
[25] J. Villarrubia, R. Dixson, S. Jones, J.R. Lowney, M.T. Postek, R.A. Allen, M.W. Cresswell, Intercomparison of SEM, AFM, and electrical linewidths, Proc. SPIE 3677 (1999) 440–587.
[26] R. Attota, R.M. Silver, M. Bishop, E. Marx, J. Jun, M. Stocker, M. Davidson, R. Larrabee, Evaluation of new in-chip and arrayed line overlay target designs, in: Proc. SPIE Microlithography, 2004.
[27] J. Seligson, M. Adel, P. Izikson, V. Levinski, D. Yaffe, Target noise in overlay metrology, Proc. SPIE 5375 (2004) 403–412.
[28] R.M. Silver, R. Attota, M. Stocker, M. Bishop, L. Howard, T. Germer, E. Marx, M. Davidson, R. Larrabee, High-resolution optical metrology, Proc. SPIE 5752 (2005) 67.
[29] R.M. Silver, R. Attota, M. Stocker, M. Bishop, J. Jun, E. Marx, M. Davidson, R. Larrabee, High-resolution optical overlay metrology, Proc. SPIE 5375 (2004) 78.
[30] R. Attota, R.M. Silver, T. Germer, M. Bishop, R. Larrabee, M. Stocker, L. Howard, Application of through-focus focus-metric analysis in high resolution optical microscopy, Proc. SPIE 5752 (2005).
[31] R.M. Silver, R. Attota, M. Stocker, J. Jun, E. Marx, R. Larrabee, B. Russo, M. Davidson, Comparison of measured optical image profiles of silicon lines with two different theoretical models, Proc. SPIE 4689 (2002) 00.
[32] T. Hu, R.L. Jones, W.-L. Wu, E.K. Lin, Q. Lin, D. Keane, S.J. Weigand, J.M. Quintana, J. Appl. Phys. 96 (2004) 1983.
[33] R.L. Jones, T. Hu, E.K. Lin, W.L. Wu, R. Kolb, D.M. Casa, P.J. Bolton, G.G. Barclay, Appl. Phys. Lett. 83 (2003) 4059.